EXAFS Observation of the Sr and Fe Site Structural Environment in SrO and Fe_2O_3-Coated SrO Nanoparticles Used as Carbon Tetrachloride Destructive Adsorbents

Shawn Decker, Isabelle Lagadic,[1] and Kenneth J. Klabunde*

Chemistry Department, Kansas State University, Manhattan, Kansas 66506

Jacques Moscovici and Alain Michalowicz*,[2]

Laboratoire de Physique des Milieux Désordonnés, Université Paris 12-Val de Marne, UFR Sciences, 62 Avenue du Général de Gaulle, 94010 Créteil Cedex, France

Received October 1, 1997. Revised Manuscript Received November 3, 1997

The Sr and Fe sites structural environment in uncoated SrO and Fe_2O_3-coated SrO nanoparticles used as destructive adsorbents in the CCl_4 decomposition have been investigated for the first time by extended X-ray absorption fine structure (EXAFS). It was found that the local structure of the Sr ions depends on the synthetic procedure used to prepare the nanoparticles. The short-range order exhibited by the sol−gel prepared SrO particles (AP−SrO) and the conventionally prepared (CP−SrO) particles is not as high as that of the commercial strontium oxide. The Sr local structure observed for the non-Fe_2O_3-coated samples after CCl_4 decomposition shows that the Sr environment is only made of Cl ions for the AP sample and made of both Cl and O ions for the CP sample, indicating that the AP−SrO sample was more reactive with CCl_4. The enhancement of the reactivity toward the CCl_4 decomposition by the iron oxide coating was evidenced from the EXAFS investigation of both the Sr and the Fe local structure after CCl_4 decomposition on Fe_2O_3-coated CP−SrO and Fe_2O_3-coated AP−SrO. It was found that the SrO inner layers are involved in the reaction since only Cl ions were detected as Sr neighbors and that no Cl ions were detected in the iron environment of this sample, suggesting that the iron oxide coating the sample surface is continuously renewed during the reaction.

Introduction

Up to now, the most extensively used technology for the disposal and the destruction of toxic chemicals, such as chlorinated hydrocarbons, has been incineration.[3] However, this method still presents some risks since toxic byproducts such as dioxins or chlorinated furans may result from an incomplete combustion.[4,5] Several alternative methods to incineration, such as catalytic processes,[6−12] have been recently investigated, focusing on a decrease in the decomposition temperature and on the production of nontoxic products. We recently reported the use of nanosized metal oxide (MgO or CaO) particles as destructive adsorbents for organophosphors[10,11] and chlorocarbon[12] compounds, through a noncatalytic and relatively low temperatures (400−500 °C)[13] process. It is based on the ability of the metal oxide to strip the heteroatom (Cl or P) from the toxic material and to immobilize it in the solid as a nontoxic substance. The volatile products are also non toxic (eq 1).

$$2CaO(s) + CCl_4(g) \rightarrow 2CaCl_2(s) + CO_2(g) \quad (1)$$

Since this surface reaction is closely related to the reaction capacity of high surface area metal oxides, a sol−gel process followed by an aerogel-hypercritical drying procedure was used to produce nanoscale MgO and CaO particles (denoted AP for aerogel prepared) with a surface area varying from 140 to 500 m^2/g. By way of comparison, the conventionally prepared metal

* To whom correspondence should be addressed.

(1) Permanent address: Chemistry Department, Oklahoma State University, Stillwater, OK 75078.

(2) Address for correspondence: Laboratoire pour l'Utilisation du Rayonnement Electromagnétique, Bat 209 D, Université Paris-Sud, 91405 Orsay Cedex, France.

(3) Exner, J. H. *Detoxification of Hazardous Waste*; Ann Arbor Science: Ann Arbor, MI, 1982.

(4) Seeker, W. R.; Koshland, C. P. *Incineration of Hazardous Waste*; Gordon and Breach Science Publishers: Philadelphia, 1992.

(5) Blakenship, A.; Chang, D. P. Y.; Jones, D. A.; Kelly, P. B.; Kennedy, I. M.; Matsumura, F.; Pasek, R.; Yang, G. *Chemosphere* **1994**, *23*, 1085.

(6) Spivey, J. J. *Ind. Eng. Chem. Res.* **1987**, *26*, 2165.

(7) Petrosius, S. C.; Drago, R. S.; Young, V.; Grunewald, G. C. *J. Am. Chem. Soc.* **1993**, *115*, 6131.

(8) Ballinger, T. H.; Yates, J. T., Jr. *J. Phys. Chem.* **1992**, *96*, *1417*.

(9) Ballinger, T. H.; Smith, R. S.; Colson, S. D.; Yates, J. T., Jr. *Langmuir* **1992**, *8*, 2473.

(10) Li, Y.-X.; Koper, O.; Atteya, M.; Klabunde, K. J. *Chem. Mater.* **1992**, *4*, 323.

(11) Li, X.-Y.; Klabunde, K. J. *Langmuir* **1991**, *7*, 1388.

(12) Koper, O.; Li, Y.-X.; Klabunde, K. J. *Chem. Mater.* **1993**, *5*, 500.

(13) Koper, O.; Wovchko, E. A.; Glass, J. A., Jr.; Yates, J. T., Jr.; Klabunde, K. J. *Langmuir* **1995**, *11*, 2054.

S0897-4756(97)00657-1 CCC: $15.00
Published on Web 01/06/1998

Scheme 1

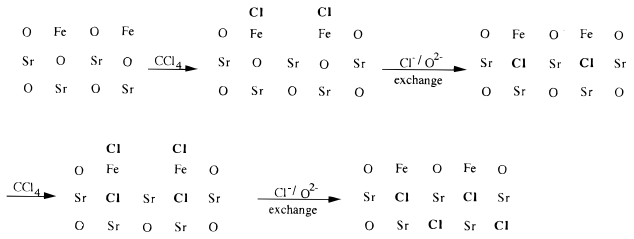

oxides (denoted CP) show a surface area ranging from 90 to 170 m^2/g, whereas the surface area of commercial metal oxides ranges only from 2 to 10 m^2/g.

The reaction of these metal oxide nanoparticles with carbon tetrachloride, chosen as a model for the adsorption−decomposition of chlorinated organic molecules, has shown that, at 425 °C, 0.23 mol of CCl_4 is decomposed per mole of CP−CaO. This capacity rises to 0.31 (mol/mol) with AP−CaO, which is much higher than on commercial CaO (less than 0.05 mol of CCl_4/mol of CaO).[14,15] To further enhance reactivities and capacities, overlayers of Fe_2O_3 were applied on these particles,[14,16] the reason being that these overlayers should give a thermodynamic advantage that could possibly lead to more efficient use of the inner layers of CaO (or MgO) in the bulk of the nanocrystals.[17] These coated particles are effectively more reactive toward CCl_4 decomposition since 0.44 mol of CCl_4 is decomposed over 1 mol of Fe_2O_3-coated CP−CaO, and this reaches the stoichiometric value 0.51 (mol/mol) on Fe_2O_3-coated AP−CaO.[14]

Thermodynamic factors alone cannot explain the reactivity of these metal oxide particles. Particle structural morphology is surely an important parameter in the different reactivity of AP samples versus CP samples. For example, the better reactivity of AP samples could be attributed to the larger porosity of these compounds (0.603 cm^3/g for AP−CaO) compared to the conventionally prepared compounds (0.474 cm^3/g for CP−CaO). That would allow the chloride ions to migrate deeper into the bulk and hence the surface would be renewed and available for further CCl_4 decomposition.[18] The enhancement of the CCl_4 decomposition over Fe_2O_3-coated particles has been explained through an ion/ion exchange process. The iron oxide would behave as though it is in a "catalytic regenerative cycle" with the metal oxide (MgO or CaO) core through an ion/ion exchange mechanism[19,20] of Cl^- and O^{2-} (Scheme 1). It was assumed that since the exchange continues into the interior of the metal oxide particle, the $Fe_2O_3-FeCl_x$ outer layer is probably mobile enough such that the surface is continuously renewed and no protective coating can form.

Therefore, particle structure is one of the important factors that controls the uncoated and coated metal oxide nanoparticles reactivity toward the CCl_4 decomposition. However, despite an in-depth investigation by gas adsorption, X-ray diffraction (XRD), X-ray photoelectron spectroscopy (XPS),[21] electron microscopy (TEM[22] and SEM), atomic force microscopy (AFM),[18] BET surface area measurements and infrared spectroscopy (IR),[13] we are still faced with a lack of information about the structure of these nanoparticles. For example, the XRD characterizations carried out on these compounds have shown the same pattern and the same bulk structure for AP and CP and were not able to detect the very small amount of Fe_2O_3 coating the metal oxide support. It is then obvious that a more revealing investigation of the alkaline-earth ion and the transition-metal ion local structure in these metal oxide nanoparticles is needed.

Herein, we report the first observation of the Sr and Fe sites structural environment in uncoated SrO and Fe_2O_3-coated SrO nanoparticles by extended X-ray absorption fine structure (EXAFS). Strontium was chosen as the absorbing alkaline-earth ion in our EXAFS experiments mostly because its K-edge energy absorption fitted with the synchrotron ring energy range better than those of calcium and magnesium. Our aim in this work is to gain information in order to clarify the following questions: (1) What is the intrinsic structural difference between the aerogel prepared (AP) and conventionally prepared (CP) samples that could explain the different reactivity toward chlorocarbon decomposition? (2) How does the Sr and Fe ion structural environment change upon reaction with CCl_4? The answers to these questions are essential to understand the enhanced reactivity of the coated metal oxide nanoparticles. The results we present below have been only qualitatively analyzed so far. The discussion is mostly based on a comparison of the Fourier transforms (not corrected for phase shift) of the EXAFS spectra.

Experimental Section

Sample Preparation. The procedure to prepare CP−SrO was based on the method already described[12] for conventionally prepared calcium oxide. Typically, 10 g of commercial SrO was slowly added to 150 mL of distilled water, stirred, and then heated to 80 °C for 2 h. The resulting strontium hydroxide was dried overnight in an oven (at least 120 °C), then calcined at 500 °C over 12 h, and held at this temperature for at least 8 h. The fine white powder, identified as SrO by powder X-ray diffraction has a specific surface area of 2.36 m^2/g. Aerogel prepared strontium oxide (AP−SrO) was prepared using the same procedure as that already described for AP−CaO.[12] Distilled methanol (230 mL) were slowly added to the strontium metal (17.48 g, 0.2 mol) in a 500 mL round-bottom flask under a flow of argon.[23] The hydrolysis of the

(14) Klabunde, K. J.; Stark, J.; Koper, O.; Mohs, C.; Park, D. G.; Decker, S.; Jiang, Y.; Lagadic, I.; Zhang, D. *J. Phys. Chem.* **1996**, *100*, 12142.

(15) Note that a ratio of 0.50 mol of CCl_4/mol of CaO is the theoretical maximum for a stoichiometric reaction.

(16) Klabunde, K. J.; Khaleel, A.; Park, D. G. *High Temp. Mater. Sci.* **1995**, *33*, 99.

(17) $2Fe_2O_3 + 3CCl_4 \rightarrow FeCl_3 + 3CO_2$

$\Delta G° = -391$ kJ/mol of CCl_4

$2FeCl_3 + 3CaO \rightarrow Fe_2O_3 + 3CaCl_2$

$\Delta G° = -506$ kJ/mol of CCl_4

(18) Koper, O.; Lagadic, I.; Klabunde, K. *J. Chem. Mater.* **1997**, *9*, 838.

(19) Stenger, H. G., Jr.; Buzan, G. E.; Berty, J. M. *Appl. Catal. B* **1993**, *2*, 117.

(20) Hedge, R. I.; Barteau, M. A. *J. Catal.* **1989**, *120*, 387.

(21) Koper, O. Ph.D. Thesis, Kansas State University, 1996.

(22) Utamapanya, S.; Klabunde, K. J.; Schlup, J. R. *Chem. Mater.* **1991**, *3*, 175.

(23) Due to the high reactivity of Sr metal, the experiments were carried out under inert atmosphere in a fume bond.

(24) Michalowicz, A. In *Logiciels pour la Chimie*; Sociéte Française de Chimie: Paris, 1991; p 102.

(25) Teo, B. K. *Inorganic Chemistry Concepts. EXAFS: Basic Principles and Data Analysis*; Springer-Verlag: Berlin, 1986; Vol. 9.

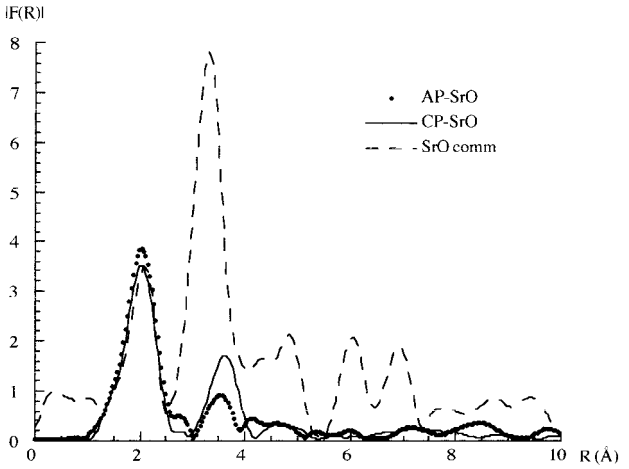

Figure 1. Fourier transform modulus spectra at the Sr edge of AP−SrO, CP−SrO, and commercial SrO (model compound).

resulting $Sr(OCH_3)_2$ was performed in distilled toluene (20 g of $Sr(OCH_3)_2$/methanol solution and 180 mL of distilled toluene). It must be emphasized that addition of the water (1.2 ml of doubly distilled water added in a drop-by-drop manner) must be very slow (10−20 min). The sol−gel mixture was hypercritically dried in a high-pressure autoclave under N_2 atmosphere (pressure = 100 psi) as described for AP−CaO.[12] The resulting fine white powdered AP−$Sr(OH)_2$ was dried overnight at 130 °C, then calcined to AP−SrO at 500 °C as described above for CP−SrO. The AP−SrO was positively identified by powder X-ray diffraction and possess a specific surface area of 8.94 m^2/g.

Iron Oxide (Fe_2O_3) Coating Process. The procedures for the Fe_2O_3 coating of CP and AP−SrO are identical. SrO (1.0 g) was placed in a Schlenk tube, and 50 mL of 8.92×10^{-3} M $Fe(acac)_3$ in tetrahydrofuran (THF) was added. The mixture was stirred overnight after flushing with argon. The THF was removed under dynamic vacuum. The resulting [$Fe(acac)_3$]−SrO orange powder was dried under dynamic vacuum for several hours and then heated from room temperature to 500 °C by ramping for 10 h and holding at the maximum temperature for 2 h. The resulting dark brown powder was identified as SrO using powder X-ray diffraction. No traces of Fe_2O_3 were detected by powder X-ray diffraction. The specific surface areas for the coated compounds were 3.22 and 9.00 m^2/g for [Fe_2O_3] CP−SrO and [Fe_2O_3] AP−SrO, respectively.

Destructive Adsorption of CCl_4 with SrO. The capability of strontium oxide to destructively adsorb carbon tetrachloride was determined via gas chromatography utilizing a pulsed reactor method. A 1/4 in. Pyrex or quartz U-tube was attached to a gas chromatograph such that a small sample of SrO (typically 50 mg) resides between the injection port and the column. The U-tube containing the sample was placed in a ceramic heater and heated to 500 °C, and 1.0 or 2.0 mL pulses of carbon tetrachloride were passed over the sample at 6 min intervals and the gaseous products/excess of CCl_4 quantified. The solid products of the reaction were determined from the powder X-ray diffraction.

All samples, even the coated compounds, readily adsorb moisture and CO_2. Therefore, they were all handled and stored under inert atmosphere after their preparation. The EXAFS studies were performed on powdered samples placed in a sealed parafilm window. This system was found to protect the samples efficiently from air exposure as we were not able to detect any change in the EXAFS spectra during the recording.

EXAFS Data Collection and Analysis. The EXAFS spectra were recorded at LURE (Laboratoire pour l'Utilisation du Rayonnement Electromagnétique), the French synchrotron radiation facility, on the storage ring DCI (1.85 GeV, 300 mA). We used an X-ray absorption spectrometer in transmission and fluorescence mode on an EXAFS III workstation with a Si311 monochomator. The detectors were low pressure (≈0.2 atm) air-filled ionization chambers for the transmission mode used at the Sr edge (≈16105 eV) for all the samples and at the Fe edge (≈7112 eV) for the iron model compounds. For the low iron loadings (<1%), we have used the fluorescence mode: the I_0 signal is still measured with an ionization chamber, while I_F is measured by a monoelement SiLi energy-sensitive solid-state detector. Each spectrum is the sum of three recordings in the range 16 060−17 060 eV in transmission mode and the sum of five recordings in the range 7090−8090 eV in fluorescence mode.

The EXAFS data analysis was performed with the "EXAFS pour le mac" programs on a Macintosh personal computer and completed in the standard way as described elsewhere. For

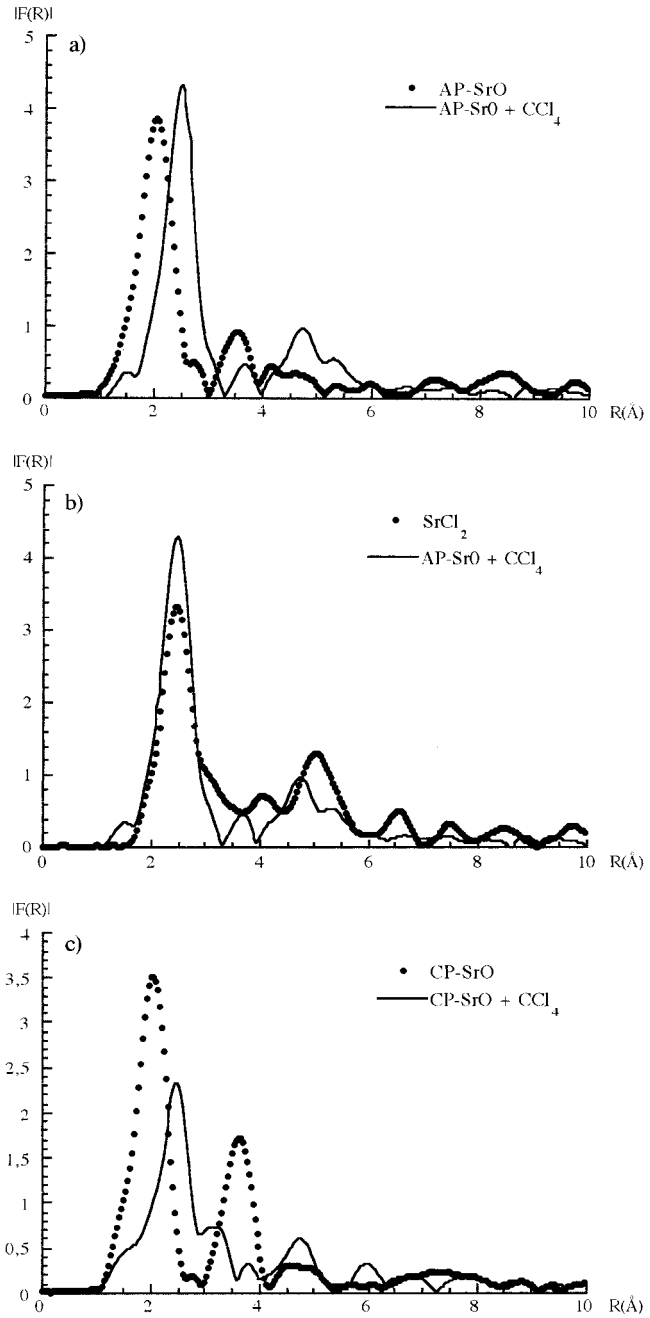

Figure 2. Comparison of the Fourier transform modulus (Sr edge): (a) AP−SrO sample before and after reaction with CCl_4. (b) AP−SrO sample after CCl_4 decomposition and $SrCl_2$. (c) CP−SrO sample before and after reaction with CCl_4.

(26) Koenisgberger, D. C.; Prins, R. *X-ray Absorption Principles, Applications and Techniques of EXAFS, SEXAFS and XANES*; Wiley: New York, 1988.

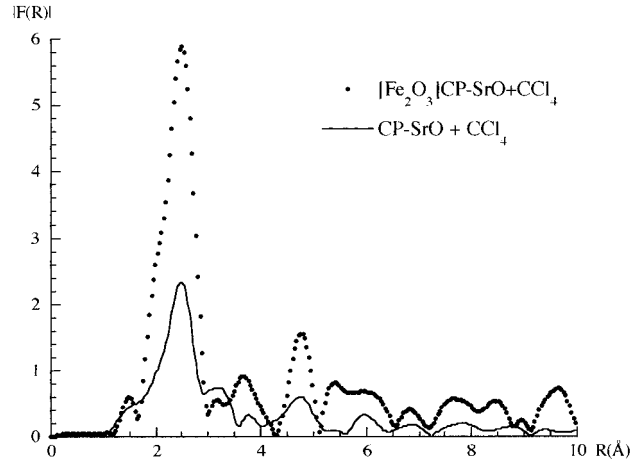

Figure 3. Comparison between the Fourier transform moduli (Sr edge) of iron oxide coated CP−SrO sample and uncoated CP−SrO sample after reaction with CCl_4.

this article, only a qualitative comparison of Fourier transform spectra has been developed and discussed. Fourier transforms were calculated using a $k^3w(k)$ window, where $w(k)$ is a Kaiser Bessel function in the range 2−12 $Å^{-1}$ for the Sr edge and 2−10 $Å^{-1}$ for the Fe edge.

Results and Discussion

Uncoated Samples. Figure 1 shows the Fourier transform modulus (without phase correction) of the EXAFS spectra of commercial SrO, CP−SrO, and AP−SrO at the Sr edge. Two major peaks corresponding to the two first shells of the Sr neighbor atoms dominate these Fourier transforms. The first-shell peak at approximately 2 Å corresponds to the oxygen atom neighbors (crystallographic distance Sr−O: 2.55 Å). The second shell peak located around 3.3 Å was identified corresponding to the strontium atom neighbors (crystallographic distance Sr−Sr: 3.609 Å). The three Fourier transform moduli are different by the magnitude of the Sr−Sr peaks, while the magnitude and the position of the Sr−O signal is unchanged. The higher magnitude of the second-shell peak for the commercial sample reflects the high crystallinity of this compound. It is then obvious that CP−SrO and AP−SrO are not as well-crystallized compared to the commercial SrO. It also appears that CP−SrO Fourier transform exhibits a second-shell peak higher than AP−SrO, suggesting that the CP compound is more ordered than its AP counterpart. This result brings up new information about the intrinsic and local morphology of these nanocrystalline metal oxides. This could not be deduced from the XRD characterization since the same bulk structure was found for AP, CP and the commercial SrO.

After reaction with CCl_4, it was expected that the local structure around the strontium atoms would be modified as the powder X-ray diffraction patterns of the reacted samples exhibit peaks characteristic of strontium chloride.[12] Figure 2a exhibits the Fourier transform of AP−SrO before and after CCl_4 reaction, and Figure 2b shows the comparison of AP−SrO after reaction with commercial $SrCl_2$. These figures confirm the above assumption: in the local environment of Sr atoms of AP−SrO after CCl_4 reaction, the oxygen atoms are replaced by chloride atoms and the first coordination sphere is comparable to that of the standard strontium

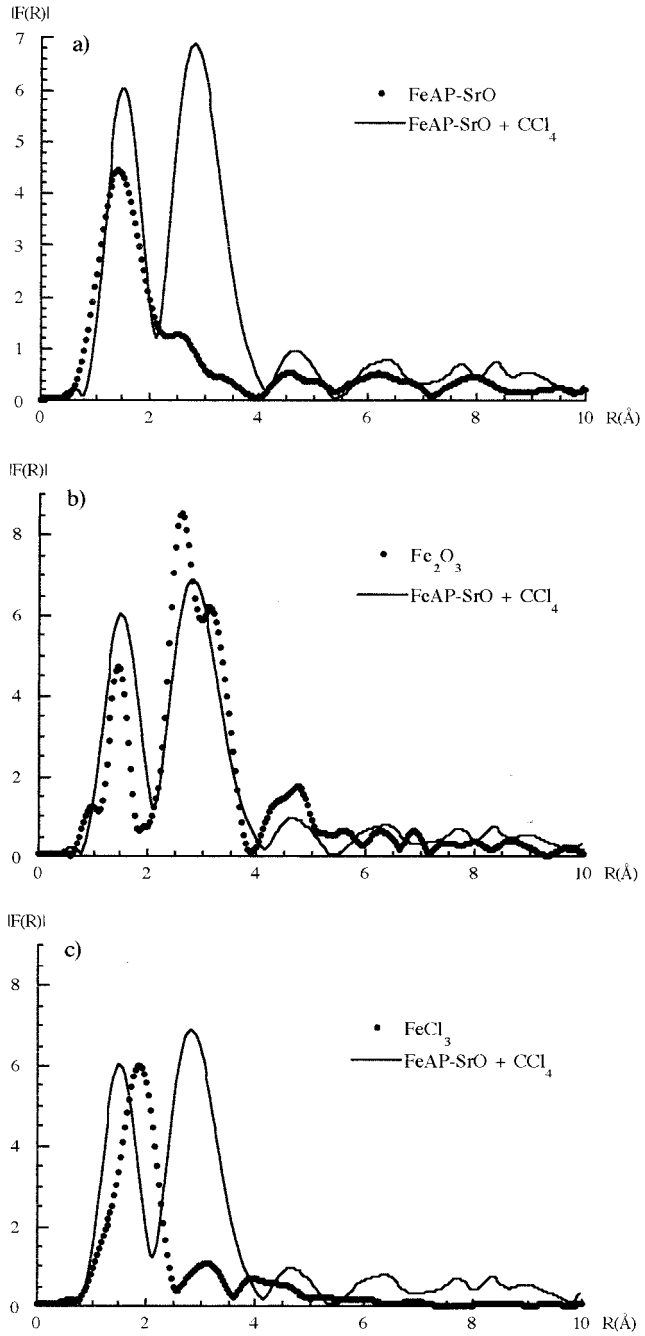

Figure 4. Comparison of the Fourier transform modulus (Fe edge): (a) $[Fe_2O_3]$AP−SrO sample before and after reaction, with CCl_4. (b) $[Fe_2O_3]$AP−SrO sample after reaction with CCl_4 and Fe_2O_3 (model compound). (c) $[Fe_2O_3]$AP−SrO sample after reaction with CCl_4 and $FeCl_3$ (model compound).

chloride. Figure 2c shows the results obtained with CP−SrO. This figure evidences an incomplete reaction, since the Sr−Cl peak is obviously smaller that in AP−SrO, and a residual signal characteristic of remaining Sr−O is present as a shoulder. The presence of oxygen in the immediate environment of the Sr ions for the reacted CP sample confirms previous observations obtained by X-ray diffraction. The XRD pattern of CP−SrO after CCl_4 decomposition exhibits both peaks corresponding to $SrCl_2$ and peaks attributed to SrO while only $SrCl_2$ peaks can be observed on the XRD pattern of AP−SrO after reaction. However, although the mixing of Sr−O and Sr−Cl is clearly demonstrated, this qualitative discussion cannot give the relative ratio of

the oxygen and chloride species.

Coated Samples. The strontium local environment after reaction of the iron coated samples with CCl_4 was also investigated. The results obtained for the compound $[Fe_2O_3]$AP−SrO after reaction was close to that found for the uncoated sample after reaction. The peak positions and magnitude are the same, suggesting that the overall environment of the strontium ions can be described the same way: in the AP−SrO after reaction, all oxygen atoms are replaced by chloride atoms. We have not come to the same conclusions for the compound $[Fe_2O_3]$CP−SrO after reaction. In this compound, the replacement of oxygen atoms by chloride atoms is more significant than for the uncoated CP sample. This can be qualitatively confirmed by the important enhancement of the Sr−Cl FT peak shown in Figure 3 and a corresponding decreasing of the Sr−O shoulder: the Sr local environment detected by EXAFS on $[Fe_2O_3]$CP−SrO + CCl_4 is comparable to those of AP−SrO + CCl_4 and of $SrCl_2$. This result would confirm the fact that the iron oxide coating enhances the use of the inner SrO core in the reaction with CCl_4 by facilitating the migration of the Cl^- ions through an exchange process of these ions with the oxygen atoms of the substrate as described in Scheme 1.

The local structure of the iron atoms was investigated for $[Fe_2O_3]$AP−SrO before and after reaction with CCl_4. Figure 4a represents the Fourier modulus comparison between $[Fe_2O_3]$AP−SrO at the iron edge before and after CCl_4 reaction. In Figure 4b, $[Fe_2O_3]$AP−SrO after reaction is compared with the Fe_2O_3 commercial compound structure. Finally, Figure 4c compares the same $[Fe_2O_3]$AP−SrO + CCl_4 spectrum with $FeCl_3$ model structure. The iron local structure of the coating before reaction can be discussed by comparing Figure 4a and Figure 4b. In Figure 4a, the EXAFS signal of iron in the coated compound before reaction exhibits clearly one Fe−O shell (around 1.5 Å corresponding to an Fe−O distance close to 1.9 Å after phase correction), and the Fe−Fe shell characteristic of the crystallized oxide is almost absent. This spectrum is characteristic of a very disordered iron oxide. After reaction, the second peak (Fe−Fe signal at 2 Å) appears and compares quite well with the commercial Fe_2O_3 spectrum, if we remember that fluorescence mode spectra of dilute species are necessarily more noisy than transmission mode spectra. From this result, we can say that the main effect of the CCl_4 reaction on the iron environment of the coating at the end of the process is to recrystallize the surface. At least, the last comparison ($[Fe_2O_3]$AP−SrO + CCl_4 versus $FeCl_3$) definitely confirms that there is no measurable Fe−Cl signal in the first iron shell. These results regarding the iron local environment for the coated samples are of great interest since no other technique was able to provide us with direct information about the structural features of the iron oxide coating.

Conclusion

The present work can be summarized as follows: (1) The local structure of the Sr ions in the SrO nanoparticle depends on the synthetic process. CP and AP−SrO samples are less crystallized than the commercial SrO sample, the AP compound being the most disordered. (2) After reaction with CCl_4, the immediate Sr environment is only made of Cl ions for the uncoated AP sample, whereas it is made of both Cl and O ions for the uncoated CP sample. (3) For the $[Fe_2O_3]$CP−SrO sample, the iron oxide coating enhances the use of the SrO inner layers in the reaction with CCl_4, as the local structure of the Sr ions for this sample is only made of Cl ions. (4) The short-range order around the iron in the iron oxide coating is much more disordered than in the pure Fe_2O_3 reference compound, since the Fe−Fe EXAFS signal is very weak. (5) After reaction with CCl_4, no Cl ions were detected in the iron environment for the $[Fe_2O_3]$AP−SrO sample, suggesting that the surface of the coated samples is continuously renewed during the CCl_4 decomposition. However, the local iron environment is rearranged since a recrystallization of the iron oxide coating occurs.

Acknowledgment. The support of the Army Research Office, the National Science Foundation, and the Centre National de la Recherche Scientifique (CNRS) is acknowledged with gratitude. The EXAFS experiments were performed at the Laboratoire pour l'Utilisation du Rayonnement Electromagnétique (LURE), University Paris-Sud, Orsay, France. The authors would like to thank Dr. Françoise Villain for her helpful assistance in the measurements of the X-ray absorption spectra as well as Jean-Blaise Brubach and Vincent Bailliez for their help during the experiments and in the data analysis.

CM970657S